

## THE MORPHOLOGY AND KINEMATICS OF THE COMPLEX POLYPOLAR PLANETARY NEBULA NGC 2440

J. A. LÓPEZ

Instituto de Astronomía, UNAM, Apdo Postal 877, Ensenada, B.C. 22800, México

AND

J. MEABURN, M. BRYCE, AND A. J. HOLLOWAY

Department of Physics and Astronomy, University of Manchester, Oxford Rd., Manchester M13 9PL, England, UK

Received 1997 June 19; accepted 1997 September 9

### ABSTRACT

Spatially resolved profiles of the H $\alpha$ , [N II] 6584 Å, and [O III] 5007 Å lines have been obtained with the Manchester echelle spectrometer combined with the 2.1 m San Pedro Mártir telescope over the planetary nebula NGC 2440. The resulting position-velocity (PV) arrays are compared with ground-based and *HST* archival imagery, revealing the complex structure that prevails in this object. This work represents the first detailed kinematical study of NGC 2440.

Several bipolar structures are shown to be emerging at different position angles from the core, as expected from bipolar, rotating, episodic outflows with different degrees of collimation. Line splitting reaches main peak to peak separations of 175 km s $^{-1}$  and 145 km s $^{-1}$  in the western and eastern main lobes, respectively. The FWZI values of the complex profiles span a range of 250 km s $^{-1}$  near the core and 150 km s $^{-1}$  in the outer regions. The nebular core is found to be a toroid expanding radially at  $\geq 22$  km s $^{-1}$ , and the systemic heliocentric radial velocity of NGC 2440 is found to be 65 km s $^{-1}$ . When combined with existing measurements of the upper limit to the angular expansion, and assuming a tilt for the axis of the central toroid of 40° in the plane of the sky, this lower limit for the expansion velocity implies a distance of  $\geq 1.45$  kpc to NGC 2440.

Puzzling kinematical features are the faint velocity components receding with radial velocity differences of 150 km s $^{-1}$  with respect to the systemic radial velocity from prominent knots at *both* ends of the brightest bipolar configuration. Scattering by dust in these knots of the line profiles from the bright nebular core is a likely explanation for this curious phenomenon.

*Subject heading:* ISM: jets and outflows — ISM: kinematics and dynamics — planetary nebulae: individual (NGC 2440)

### 1. INTRODUCTION

NGC 2440 has always been considered to be a typical bipolar planetary nebula (PN). However, its morphology is far from typical. NGC 2440 is characterized by two main bipolar structures and an apparent symmetric “jet” along the brighter bipolar configuration. Kinematical evidence for polypolar, as opposed to simple bipolar, structures in PNs have been noted before (e.g., for NGC 6302 by Meaburn & Walsh 1980 and Barral, Cantó, & Meaburn 1982; for Mz 3 by Meaburn & Walsh 1985, and see Manchado, Stanghellini, & Guerrero 1996). It was Kaler & Aller (1974) who first suggested, in a schematic interpretation of the basic structure of NGC 2440, that outflows in different directions were emerging episodically from the core within bipolar configurations. Furthermore, Pascoli (1990) described the morphology of NGC 2440 as the consequence of “two ejections with precession of the symmetry axis.” The presence of multiple lobes, or mildly collimated outflows, together with the presence of a symmetric “jet,” could suggest that a bipolar, rotating, episodic jet (BRET) may be at work in this object.

High-velocity collimated outflows, with morphologies that indicate episodic ejections from rotating sources, have been found in a number of PNs (e.g., Miranda & Solf 1992; López, Meaburn, & Palmer 1993; López, Vázquez, & Rodríguez 1995; López et al. 1997; López 1997 and references therein). These discoveries present a dilemma, since the driving agents for two-sided jets are generally thought to be

embedded in accretion disks, and the latter are not established components of PNs. Consequently, explanations for the formation of collimated outflows in planetary nebulae have been sought in models of close binary systems that undergo a common envelope phase and eventually result in the formation of an accretion disk (cf. Soker & Livio 1994).

Cliffe et al. (1995) have presented numerical simulations of a BRET that reproduces the main morphological features observed. More recently, Livio & Pringle (1996) have considered the effects of radiation-induced, self-warping instabilities in accretion disks and concluded that the time-scales on which these warping instabilities occur are of the right order to produce wobbling (if not rotating) symmetric jets. Also, recent numerical MHD simulations by Różyczka & Franco (1996) and García-Segura (1997) show that diverging stellar winds from single stellar cores with frozen-in toroidal magnetic fields may evolve into bipolar collimated outflows in PNs. Różyczka & Franco (1996) also speculate that the changes in the direction of the outflows, as observed in BRETs, may be due to temporary misalignments of the stellar rotational and magnetic axes.

The physical conditions in NGC 2440 have been extensively studied in the past. It is a very high excitation object, with ionic abundances that indicate a PN type I classification. As is usual for PNs, its distance is very uncertain. Bassgen, Diesch, & Grawein (1995) compute 500 pc from a two-dimensional cylindrical model applied to monochromatic images and low-dispersion spectra. On the other

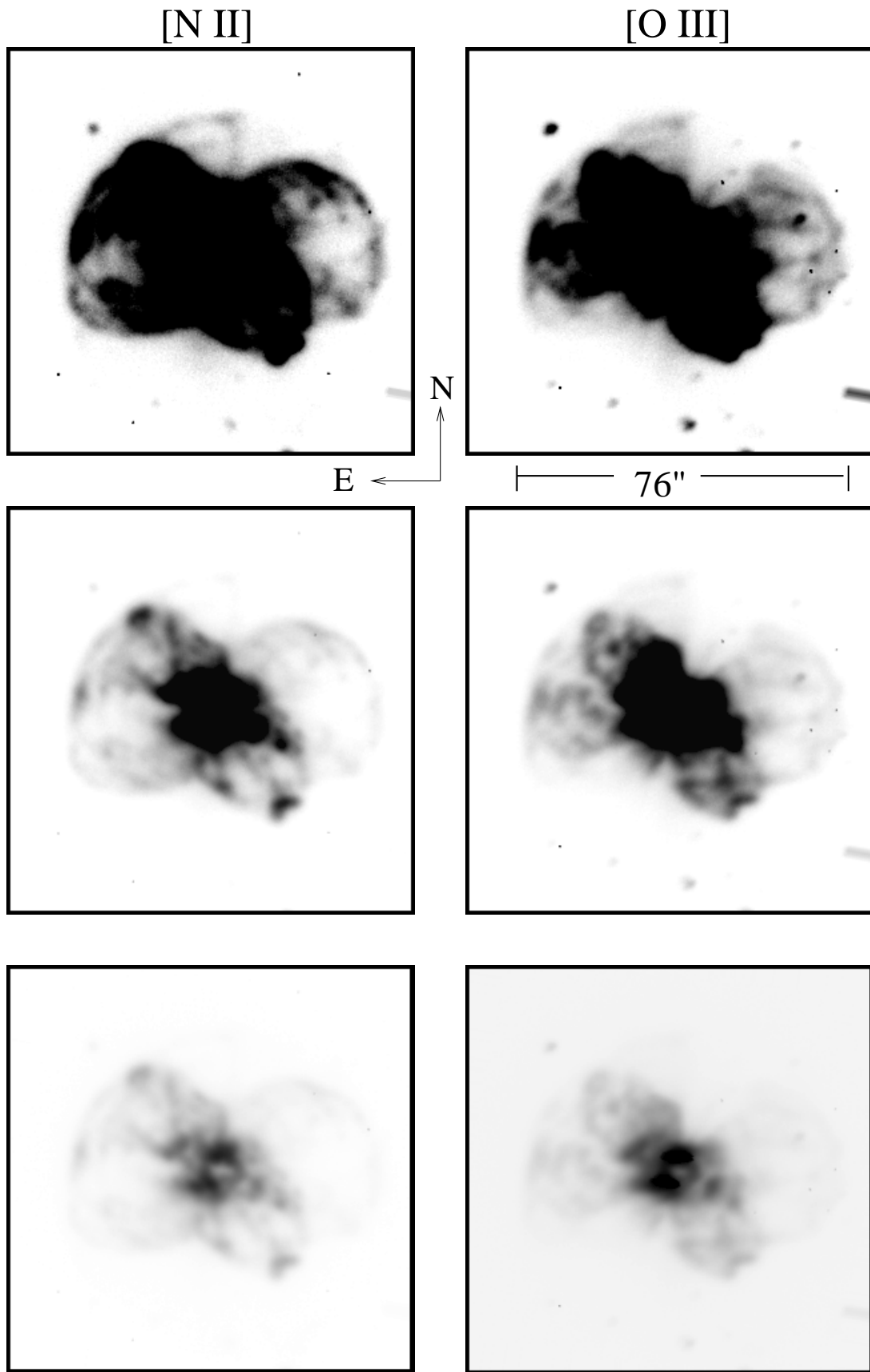


FIG. 1.—Logarithmic negative representations of the images of NGC 2440 in the light of [N II] 6584 Å (*left column*) and [O III] 5007 Å (*right column*). In both cases, prints of different depth are shown to reveal different aspects of the morphology.

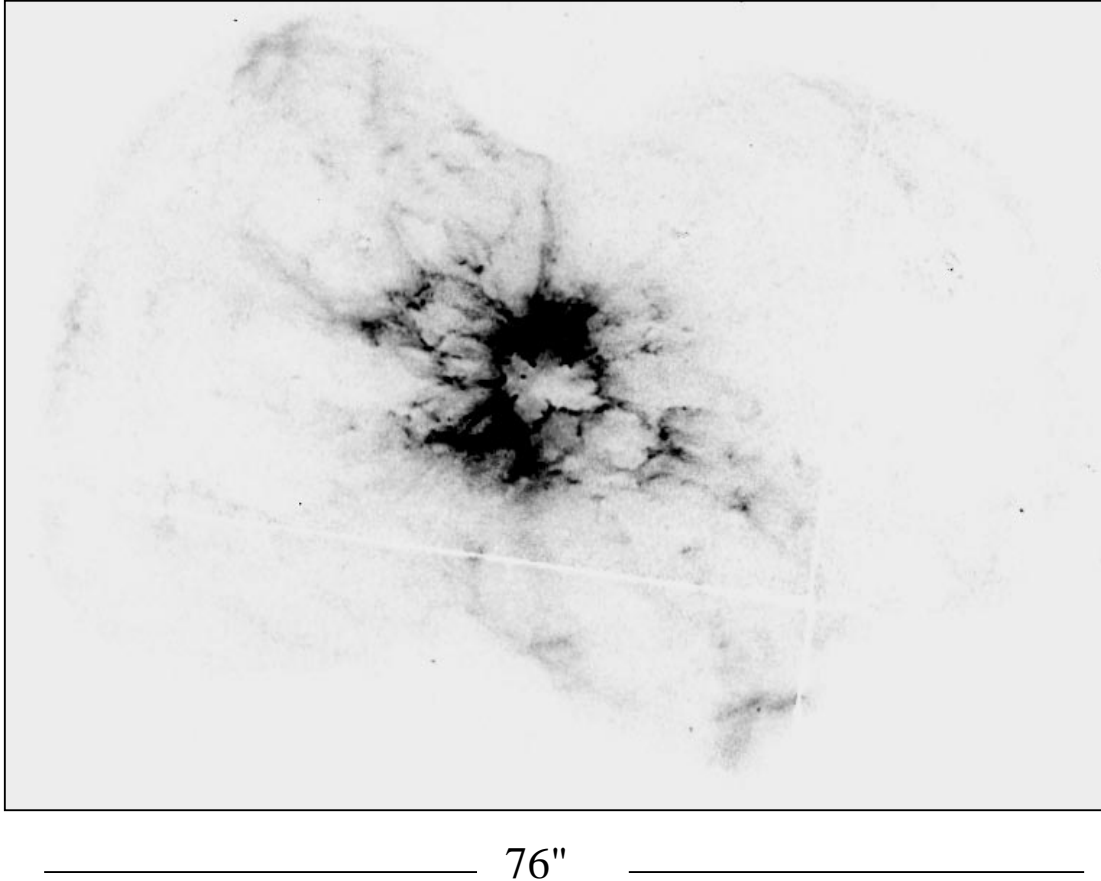


FIG. 2.—A broadband F622W pre-COSTAR *HST* image of NGC 2440 deconvolved with the LUCY algorithm to give a  $0.^{\prime\prime}1$  resolution

hand, Hajian & Terzian (1996) have used two-epoch VLA expansion-parallax measurements to obtain a lower limit to the distance of NGC 2440 of 1.1 kpc. The latter authors refer to the existing measurements of the expansion velocity in the inner regions of NGC 2440, pointing out the lack of consistency and the need for spatially resolved observations.

In the present paper, we present the first detailed kinematical study of the lobes, the inner regions near the core, and the possible jets in NGC 2440. These observations are then compared with ground based and *Hubble Space Telescope* (*HST*) archival images.

## 2. OBSERVATIONS AND RESULTS

Narrowband images of NGC 2440 were obtained on 1995 February 4 with the 2.1 m San Pedro Mártir telescope. The images in the light of [N II] 6584 Å (10 Å HPBW) and [O III] 5007 Å (52 Å HPBW) are shown in Figure 1. A Tektronix CCD with  $1024 \times 1024$   $24 \mu\text{m}$  ( $\equiv 0.^{\prime\prime}3$ ) square pixels was the detector. A broadband F622W *HST* pre-COSTAR image, retrieved from the public archive (program 1108, P. I. Westphal, observation date 1992 February 6) is shown in Figure 2. This has been deconvolved using the LUCY routine with STSDAS. A satisfactory result was achieved with a nominal  $0.^{\prime\prime}1$  resolution in the central bright regions. An enlargement of the central region of NGC 2440 from this image is presented in Figure 3.

The long-slit spectral observations were obtained with the Manchester echelle spectrometer (MES; Meaburn et al. 1984), combined with the f/7.9 focus of the 2.1 m San Pedro

Mártir UNAM telescope in two separate runs (1995 October 22 and 1996 April 17). This spectrometer has no cross-dispersion. The same Tektronix CCD was the detector. Two times binning was employed in both the spatial and spectral dimensions. Consequently, 512 increments, each  $0.^{\prime\prime}60$  long, gave a total projected slit length of  $5.12$  on the sky. Seeing varied between  $1.^{\prime\prime}2$  during these observations. The spectra were calibrated to  $\pm 1 \text{ km s}^{-1}$  accuracy against that of a Th/Ar arc lamp. The slit was always orientated east-west, with integration times ranging from 1800 s for the outer regions to 60 s for the core.

Three sets of long-slit spectral observations were made. In the first, a filter of 90 Å bandwidth was used to isolate the 87th order containing the H $\alpha$  and [N II] 6584 Å nebular emission lines. Here the single slit was  $150 \mu\text{m}$  wide ( $\equiv 10 \text{ km s}^{-1}$  and  $1.^{\prime\prime}9$ ). For the second and third sets, a five-element multislit was used (with each slit  $70 \mu\text{m}$  wide  $\equiv 6 \text{ km s}^{-1}$  and  $0.^{\prime\prime}9$ ), but with 10 Å and 70 Å bandwidth filters isolating the [N II] 6584 Å and [O III] 5007 Å lines in the 84th and 114th orders, respectively. The slit positions a–i, where significant profiles of some of these lines were obtained, are shown in Figure 4 against a sketch of the nebula from the images in Figure 1. These positions are particularly well known because a plane mirror can be inserted into the beam before the echelle grating of MES, permitting an image to be taken of the slit against that of the field being observed (see Meaburn et al. 1984). Gray-scale representations of some of the resulting PV arrays of [N II] 6584 Å or [O III] 5007 Å profiles for slit positions a–i are shown in Figures 5a–5i. The spatial extent of these dis-

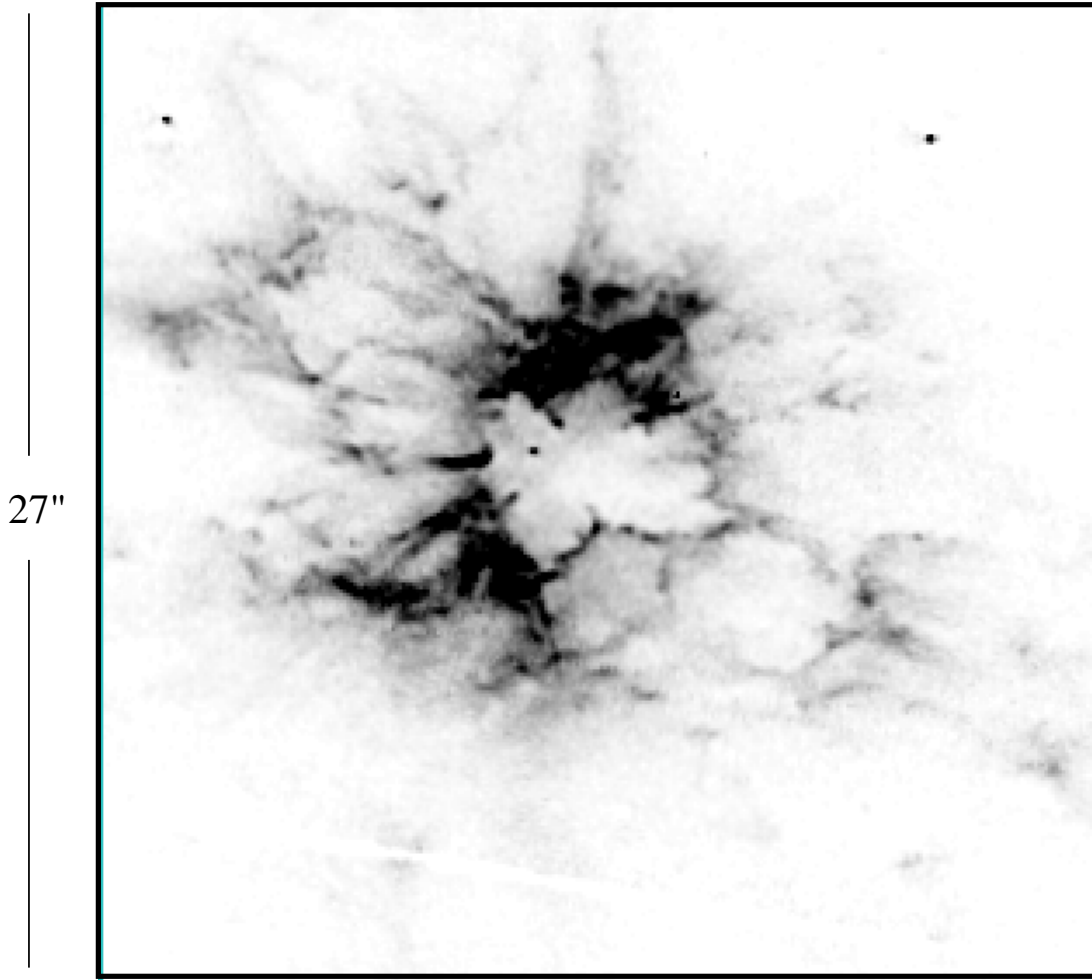


FIG. 3.—Enlargement of the core of NGC 2440 from the *HST* image in Fig. 2

plays corresponds to the 76" lengths of the slits marked in Figure 4. Individual velocity features from the PV arrays e and g are illustrated in detail in the gray-scale plus contour maps in Figures 6 and 7.

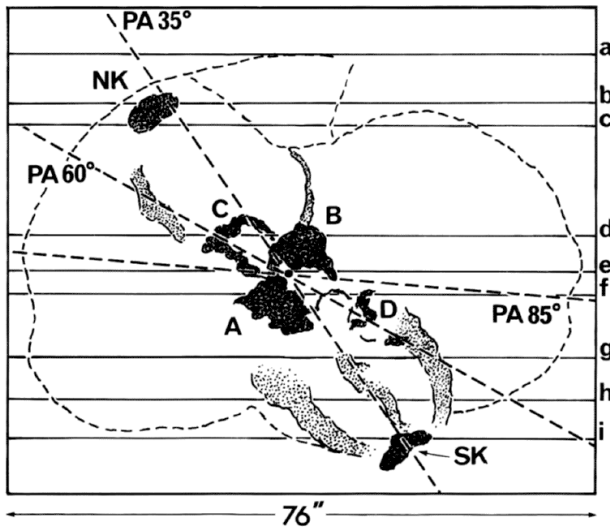


FIG. 4.—MES slit positions a-i marked against a sketch of NGC 2440. The position angles of the axes of the three bipolar lobes are also indicated. Core knots A-D are marked, as are the knots NK and SK at the extremities of the P.A. 35° bipolar lobes.

### 3. DISCUSSION

#### 3.1. Morphology

An appreciation of the intricate morphology of NGC 2440 is necessary for a better understanding of its kinematics. The images in Figure 1 show the complex morphology of NGC 2440, characterized by two bipolar structures whose main axes of symmetry are tilted in the plane of the sky by  $\sim 50^\circ$  with respect to each other (P.A.  $85^\circ$  and  $35^\circ$ , respectively; see Fig. 4). Along the brighter of these two bipolar structure, P.A.  $35^\circ$ , a symmetric jet-like feature, particularly bright in the [N II] 6584 Å image in Figure 1, emerges from the core, culminating in two well-defined knots (NK and SK in Fig. 4) at the opposite borders of the P.A.  $35^\circ$  lobes. Knot SK in Figure 4 is clearly a convex arc from the point of view of the central star, as revealed in the *HST* image in Figure 2.

Differences worth noticing between the [O III] 5007 Å and the [N II] 6584 Å images in Figure 1 are the bright, symmetric [O III] 5007 Å condensations located halfway between the core and the tips of the jet-like structure. Also, a bright [N II] 6584 Å knot located on the eastern edge of the P.A.  $85^\circ$  lobes is preceded by a twisted filament (probably a chain of knots) visible only in the [O III] 5007 Å image in Figure 1.

The line intensity ratio maps of NGC 2440 and their analysis by Richer, Martin, & Marshall (1991) demonstrate

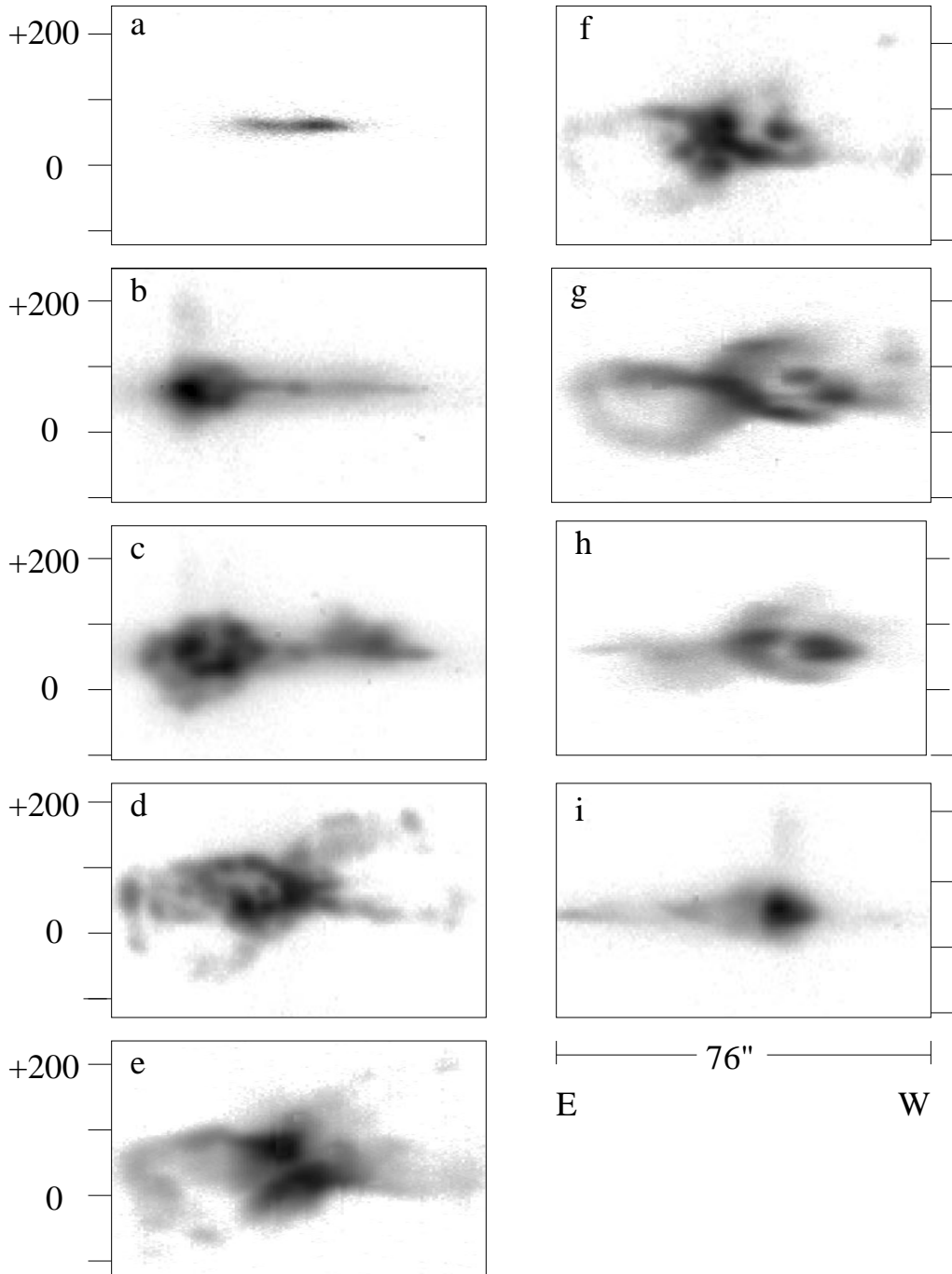


FIG. 5.—Negative gray-scale representations of the position-velocity arrays of line profiles for slit positions a–i (marked in Fig. 4) are shown in (a)–(i), respectively. The spatial extent ( $76''$ ) is exactly as shown in Fig. 4. [O III] 5007 Å profiles are shown in (e); all others are for the [N II] 6584 Å line.

further the complexity of physical structure within this object. They suggest the presence of small, optically thick clumps embedded in a diffuse, optically thin medium surrounding the core. These clumps then produce varying optical depths along different lines of sight. This detailed morphology is consistent with the H<sub>2</sub> observations by Reay, Walton, & Atherton (1988) and more recent observations of Latter et al. (1995) and Kastner et al. (1996), in which the bright H<sub>2</sub> emission near the core is interpreted as originating in collisionally excited molecular material distributed in a toroidal geometry.

Comparison of the images in Figures 1, 2, and 3 is revealing. The enlargement of the broadband *HST* image in

Figure 3 clearly shows the central star surrounded by a seemingly toroidal configuration with multiple radial filaments streaming outward. Furthermore, the symmetric “knots” labeled C and D in Figure 4 have the appearance in Figures 2 and 3 of a farther, and presumably younger, bipolar outflow along P.A. 60°.

Some of the structures in the enlarged *HST* image in Figure 3 are reminiscent of those expected for mass-loaded flows driven by a fast wind from the central star as this ablates subarcsecond condensations within the regions marked C and D in Figure 4. In this respect, there is a strong morphological similarity to structures discovered by Borkowski, Harrington, & Tsvetanov (1995) in the core of

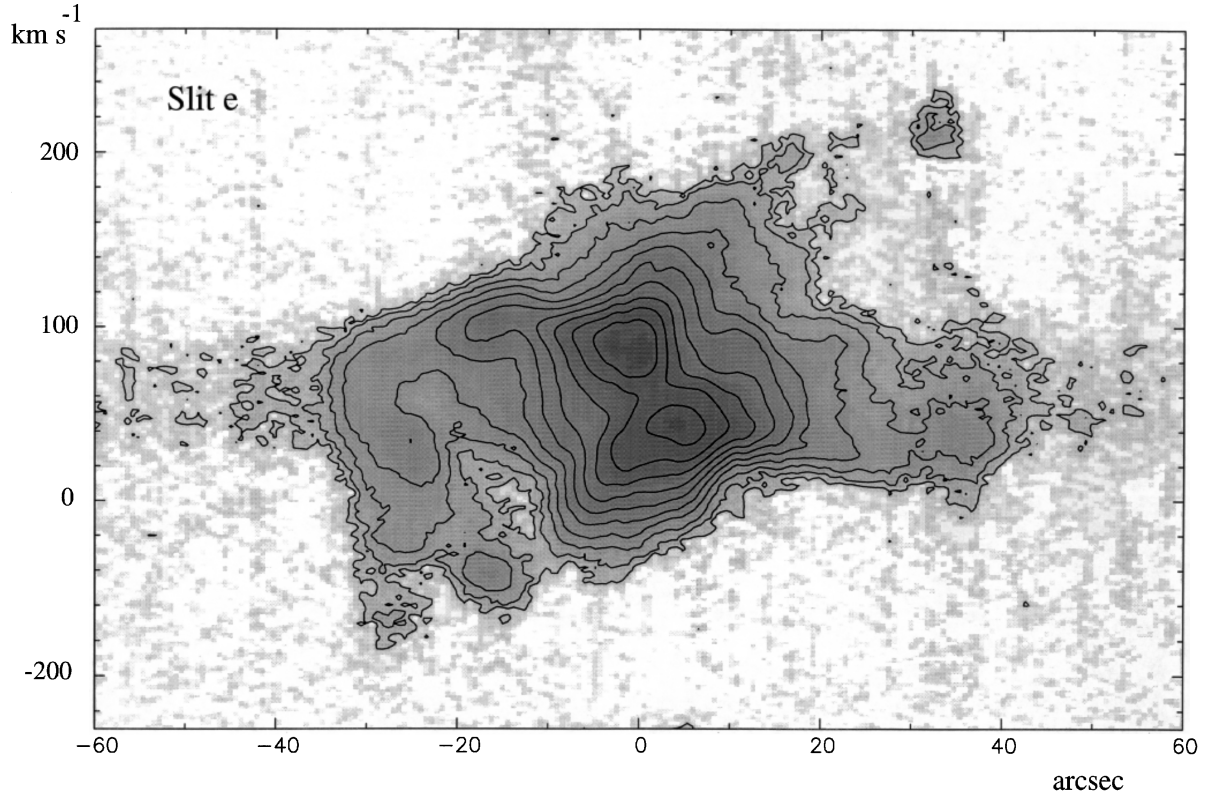


FIG. 6.—A continuum-subtracted,  $\log_{10}$  gray-scale/contour map of the [O III] 5007 Å PV array in Fig. 5e (for slit e in Fig. 4), covering the core of NGC 2440. The  $\log_{10}$  value of the lowest contour is 0.8 above the background zero. After that, the contour intervals are equally spaced on a logarithmic scale to a maximum value of  $\log_{10} = 4.02$ .

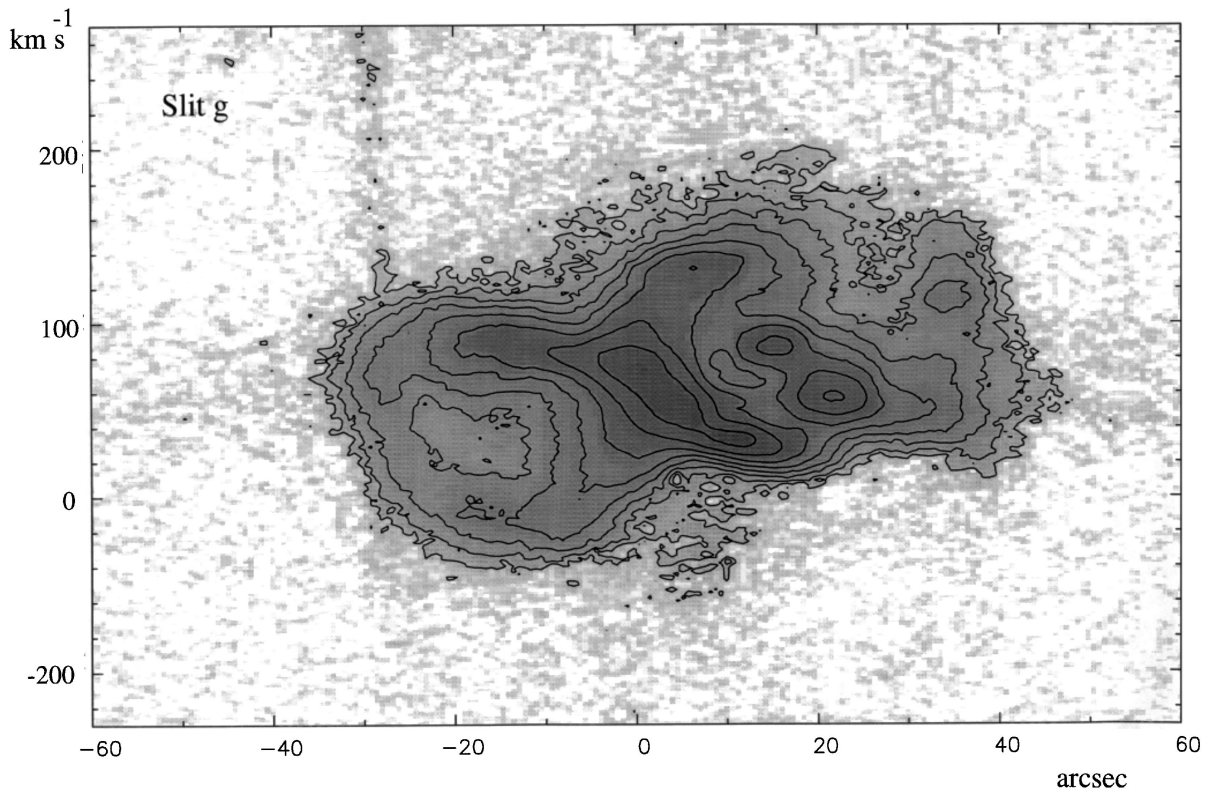


FIG. 7.—As for Fig. 6, but for slit g (see Figs. 4 and 5g). Here, the lowest contour is for  $\log_{10} = 0.75$ , and the highest is 3.

the hydrogen-deficient PN Abell 30 (see also Meaburn & López 1996). The regions labeled A and B in Figure 4 now appear in Figures 2 and 3 to be dense concentrations of knots and filaments on the inside edge of an irregular toroidal shell surrounding the central star. Thus, this pre-COSTAR *HST* image confirms previous suggestions about the structure of the core of NGC 2440 that were based solely on optical and IR ground-based observations.

The morphology of NGC 2440 can then be summarized as follows. It is composed of at least two and possibly three bipolar structures; the largest along P.A.  $85^\circ$ , the bright lobes along P.A.  $35^\circ$ , and what could be the most recent pair, defined by the regions C and D, at P.A.  $60^\circ$ .

A bipolar, jet-like feature, detected only in the narrow-band San Pedro Martir [N II] 6584 Å image, appears to be closely associated with both the P.A.  $35^\circ$  bipolar lobes and the bright knots at each extremity, NK and SK. The central star is surrounded by a toroidal structure.

### 3.2. Kinematics

The presence of multiple bipolar lobes, at different position angles and with varying degrees of collimation, suggests a history of episodic ejections along changing axes within NGC 2440. The morphology of NGC 2440 must be considered in the light of the complex motions found in this peculiar object.

#### 3.2.1. P.A. $85^\circ$ Bipolar Lobes

The [O III] 5007 Å profiles from slit e in Figure 5e and Figure 6, from the bright core of NGC 2440, are centered on  $V_{\text{HEL}} \sim +65 \text{ km s}^{-1}$ , which will be taken as the mean systemic radial velocity of the nebula. It is then apparent from Figures 5d–5g that the western side of the P.A.  $85^\circ$  bipolar lobes is receding, while the eastern side is approaching. The largest peak-to-peak velocity differences for the western and eastern lobes in Figure 5d (slit d) are  $145 \text{ km s}^{-1}$  and  $135 \text{ km s}^{-1}$ , respectively. Likewise, those for slit f, Figure 5f, are  $175 \text{ km s}^{-1}$  and  $145 \text{ km s}^{-1}$ . A simple model can now be used to estimate the orientation of the axis of the P.A.  $85^\circ$  bipolar lobes with respect to the sky as well as the speed of the outflowing material. First, the opening angle (the angle subtended by an individual lobe diameter to the central star) of the P.A.  $85^\circ$  lobes can be seen in Figure 1 to be  $\approx 80^\circ$ . The velocity vectors for the outflowing material of the lobes must have components both parallel and perpendicular to the lobe walls. If it is assumed that the outflows are always along radial directions from the central star, and that, from the PV arrays in Figures 5d and 5f, the far wall of the eastern lobe and near wall of the western lobe are both nearly in the plane of the sky, then the axis of the P.A.  $85^\circ$  bipolar lobe is tilted  $\approx 40^\circ$  to the plane of the sky, and the outflow speed in this radial direction near the center of each lobe is  $\approx 150 \text{ km s}^{-1}$ , i.e., nearly equal to the maximum difference in radial velocities of the two velocity components over each lobe.

A faint wedge-shaped feature is present in the northern part of the nebula (Fig. 1), which seems separate from the P.A.  $85^\circ$  lobes. The edge of this is covered by slit a (Fig. 4), where a narrow component on the systemic radial velocity is found (Fig. 5a) that continues along the next slit position b. In a deeper representation of an [O III] 5007 Å PV array, not shown here, there is a faint, diffuse, receding component along slit b extending out to  $V_{\text{HEL}} = 200 \text{ km s}^{-1}$ , leaving the interpretation of this wedged feature somewhat uncertain.

#### 3.2.2. P.A. $35^\circ$ Bipolar Lobes

The bright P.A.  $35^\circ$  lobes (see Fig. 4) can be traced in the PV arrays for slits b, c, g, h, and i (Figs. 5b, 5c, 5g, and 5i; see also Fig. 7) as “velocity ellipses” as the slit crosses them. An approximately circular section for these lobes is indicated, but with a component of radial expansion. The two velocity components for the northeastern lobe are at  $V_{\text{HEL}} = 30$  and  $105 \text{ km s}^{-1}$ , respectively (slit c, Fig. 5c) and for the southwestern lobe at 29 and  $95 \text{ km s}^{-1}$ , respectively (slit g, Fig. 7). Remarkably, this splitting for the P.A.  $35^\circ$  lobes on both sides of the nebular core is nearly centered on the systemic heliocentric radial velocity of  $65 \text{ km s}^{-1}$ . The axis of the lobes must then be nearly in the plane of the sky. The opening angle of the P.A.  $35^\circ$  lobes is only  $\approx 30^\circ$  (see Fig. 1), and with the splitting of  $\approx 70 \text{ km s}^{-1}$  and the bipolar lobe axis in the plane of the sky, the outflow speed could be as high as  $\approx 135 \text{ km s}^{-1}$ , i.e.,  $35/\cos 75^\circ \text{ km s}^{-1}$ , if the flow is always along a radial direction from the central star.

Conspicuous components of the P.A.  $35^\circ$  bipolar lobes are also the bright knots at both ends (NK and SK) and the filaments connecting them to the core. In the southwest lobe, the PV array for slit g (see Fig. 7) presents a velocity “knot”  $16''$  west of the center with  $V_{\text{HEL}} = 86 \text{ km s}^{-1}$ , which must be produced by the filament connecting SK with the core (Figs. 1 and 4), whereas a second velocity knot in the same array at  $22''$  west of the center and with  $V_{\text{HEL}}$  near the systemic radial velocity must correspond to the edge of this P.A.  $35^\circ$  lobe. Simply from the imagery in Figure 1, it is tempting to interpret this filament as a highly collimated outflow (i.e., a jet) along the axis of the lobe, but the present data can not discount the possibility of a filamentary structure in the surface of the far side of the lobe.

Slits b and i intersect the bright [N II] 6584 Å knots (NK and SK, respectively, in Fig. 4) on the edges of the P.A.  $35^\circ$  bipolar lobe. Both NK and SK can be seen to have nearly the systemic radial velocity. Presumably, their direction of motion is nearly in the plane of the sky, which is consistent with the interpretation that they are apices of the P.A.  $35^\circ$  bipolar lobes. In addition, faint, receding velocity components of  $\approx 150 \text{ km s}^{-1}$  in extent are found associated with both knots NK and SK (see Figs. 4, 5b, and 5i). These redshifted components are also present in [O III] 5007 Å profiles of the knots. A likely explanation for this puzzling phenomenon is to consider that the bright line emission from the nebular core is being scattered by dust associated with these outflowing knots, whose velocities from the central star are similar to those of the P.A.  $35^\circ$  lobes. An expanding scatterer would redshift the lines from a central source whatever the angle of the observer’s sightline, as in the models of Henney (1994). The H<sub>2</sub> imagery at  $2.12 \mu\text{m}$  of NGC 2440 by Kastner et al. (1996) and Latter et al. (1995) reveal clearly prominent emission from NK and SK, indicative of dense, cool, and probably dusty conditions in these knots and supporting the expanding scatterer interpretation. A similar situation has been found in the bipolar planetary nebula M 2–9 by Solf (1993) and Schwarz et al. (1997). Spectropolarimetry or radio recombination line observations should distinguish between intrinsic and reflected emission from the NK and SK system.

#### 3.2.3. P.A. $60^\circ$ Bipolar Lobes

The filamentary P.A.  $60^\circ$  lobes appear in Figures 2 and 3 to be the latest rotated outflow that originally may have generated the P.A.  $35^\circ$  lobes. Slits d and f (Figs. 5d and 5f)

cross over the regions marked as C and D in Figure 4, which would correspond to the opposite sides of this bipolar structure. Slit d (Fig. 5d) intersects region C at an angle to its axis. Here, the main velocity components at maximum expansion are located at  $33 \text{ km s}^{-1}$  and  $99 \text{ km s}^{-1}$ . Incidentally, these values coincide with those reported by Meatheringham, Wood, & Faulkner (1988) from the [O II] line emission, indicating that their data was probably taken from this zone in the nebula. Region D is represented in slit f (Fig. 5f) as a velocity “knot” located near the systemic radial velocity. Presumably, then, the axis of these P.A.  $60^\circ$  lobes is also nearly in the plane of the sky. The main evidence for these P.A.  $60^\circ$  lobes is their orthogonality to the plane of the central torus; however, the present kinematical data do not cover them in sufficient spatial detail to permit any definite statement about their kinematics. A closely separated set of long-slit observations over the nebular core are now required to confirm the existence of these lobes as kinematically separate from the other bipolar outflows.

### 3.2.4. Core

The manifestation of the core (knots A & B in Fig. 4) as a radially expanding toroid are immediately apparent. Within this interpretation, the PV array for slit e in Figure 6 can now be used along with the upper limit of angular expansion of  $4.4 \text{ mas yr}^{-1}$  found by Hajian & Terzian (1996) for knots A and B in Figure 4 to make a better estimate of the distance to NGC 2440. Slit e crosses the core between these knots.

The two bright maxima in the center of the PV array in Figure 6 are separated by a radial velocity difference of  $44 \text{ km s}^{-1}$  and displaced by nearly equal amounts on either side of the systemic radial velocity of  $65 \text{ km s}^{-1}$ . These maxima, then, appear to be manifestations of the receding and approaching sides of the central, radially expanding toroid whose edges, viewed tangentially, are marked A and B in Figure 4. If the axis of the toroid is in the plane of the sky, then its expansion velocity is simply  $22 \text{ km s}^{-1}$ , and a distance to NGC 2440 of  $\geq 1.1 \text{ kpc}$  is indicated, in agreement with the lower limit given by Hajian & Terzian (1996) when combined with their upper limit to the angular expansion. However, if this axis is tilted  $40^\circ$  with respect to the plane of the sky (as estimated in § 3.2.1 for the P.A.  $85^\circ$  lobes), then an expansion velocity of  $29 \text{ km s}^{-1}$ , i.e.,  $22/\cos 40^\circ$ , is indicated, and the lower limit for the distance becomes  $\geq 1.45 \text{ kpc}$ .

- Barral, J., Cantó, J., & Meaburn, J. 1982, MNRAS, 199, 817
- Bassgen, M., Diesch, C., & Grewing, M. 1995, A&A, 297, 828
- Borkowsky, K. J., Harrington, J. P., & Tsvetanov, Z. I. 1995, ApJ, 449, L143
- Cliffe, J. A., Frank, A., Livio, M., & Jones, T. W. 1995, ApJ, 447, L49
- García-Segura, G. 1997, ApJ, 489, L189
- Hajian, A. R., & Terzian, Y. 1996, PASP, 108, 419
- Henney, W. J. 1994, ApJ, 427, 288
- Kaler, J. B., & Aller, L. H. 1974, PASP, 86, 635
- Kastner, J. H., Weintraub, D. A., Gatley, I., Merrill, K. M., & Probst, R. G. 1996, ApJ, 462, 777
- Latter, W. B., Kelly, D. M., Hora, J. L., & Deutsch, L. K. 1995, ApJS, 100, 159
- Livio, M., & Pringle, J. E. 1996, ApJ, 465, L55
- López, J. A., Meaburn, J., & Palmer, J. A. 1993, ApJ, 415, L135
- López, J. A., Vázquez, R., & Rodríguez, L. F. 1995, ApJ, 455, L63
- López, J. A. 1997, in IAU Symp. 180, Planetary Nebulae, ed. H. J. Habing & H. Lammers (Dordrecht: Kluwer)
- López, J. A., Meaburn, J., Bryce, M., & Rodríguez, L. F. 1997, ApJ, 475, 705

## 4. CONCLUSIONS

The spatially resolved, kinematical information presented here, together with the ground-based and *HST* imagery, have proven crucial to the understanding of the nature of the various interactions occurring in the core and outer regions of NGC 2440. At least two and possibly three outflowing bipolar structures located at different position angles (P.A.  $85^\circ$ ,  $60^\circ$ , and  $35^\circ$ ) are present in this object. Whereas the P.A.  $85^\circ$  lobes are tilted by  $40^\circ$ , the other two bipolar structures seem to lie on or very close to the plane of the sky

The knots NK and SK (Fig. 3) at the tips of the P.A.  $35^\circ$  lobes are bright in low-ionization species and H<sub>2</sub>, indicating that they have dense, cold cores. Both have redshifted components, and this apparent anomalous kinematical behavior could be explained by a bipolar outflow perpendicular to the line of sight, which scatters the optical emission lines from the bright core.

The core contains a toroid expanding at  $22 \text{ km s}^{-1}$  if its axis is in the plane of the sky, or up to  $29 \text{ km s}^{-1}$  if tilted by up to  $40^\circ$ . These values, combined with the lower limit of the angular expansion–parallax VLA observations derived by Hajian & Terzian (1996), indicate lower limits for the distance to NGC 2440 of  $\geq 1.1 \text{ kpc}$  or  $\geq 1.45 \text{ kpc}$ , respectively.

The collimating agent of the various bipolar structures in NGC 2440 seems to have suffered transformations with time, given the different orientations and degrees of collimation of the outflows found here. A dynamical interpretation of the origin and evolution of these outflows still requires further investigation. However, as with other cases of BRETs in PNs (e.g., López 1997 and references therein), the apparent variations of the main symmetry axis over the course of a succession of seemingly episodic bipolar outbursts has had a profound effect on the shaping of this nebula.

We wish to thank the staff of the San Pedro Mártir Observatory for their excellent assistance during these observations. J. A. L. gratefully acknowledges continuous support from CONACYT and DGAPA-UNAM. J. M. is grateful to PPARC for funding the conversion of the Manchester echelle spectrometer for use on the San Pedro Mártir telescope.

## REFERENCES

- Manchado, A., Stanghellini, L., & Guerrero, M. 1996, ApJ, 466, L95
- Meaburn, J., & López, J. A. 1996, ApJ, 472, L47
- Meaburn, J., & Walsh, J. R. 1980, MNRAS, 193, 631
- Meaburn, J., & Walsh, J. R. 1985, MNRAS, 215, 761
- Meaburn, J., Blundell, B., Carling, R., Gregory, D. E., Keir, D. F., & Wynne, C. G. 1984, MNRAS, 210, 463
- Meatheringham, S. J., Wood, P. R., & Faulkner, D. J. 1988, ApJ, 334, 862
- Miranda, L. F., & Sofle, J. 1992, A&A, 260, 397
- Pascoli, G. 1990, A&A, 232, 184
- Reay, N. K., Walton, N. A., & Atherton, P. D. 1988, MNRAS, 232, 615
- Richer, M. G., McCall, M. L., & Martin, P. G. 1991, ApJ, 377, 210
- Rózyczka, M., & Franco, J. 1996, ApJ, 469, L127
- Schwarz, H. E., Aspin, C., Corradi, R. L. M., & Reipurth B. 1997, A&A, 319, 267
- Soker, N., & Livio, M. 1994, ApJ, 421, 219
- Solf, J. 1993, in Stellar Jets and Bipolar Outflows, ed. L. Errico & A. A. Vitcone (Dordrecht: Kluwer), 235